CHEMISTRY
AN ASIAN JOURNAL
www.chemasianj.org

Accepted Article

Title: Kinetic and Theoretical Studies on Ni(0)/N-Heterocyclic Carbene-Catalyzed Intramolecular Alkene Hydroacylation

Authors: Yoichi Hoshimoto; Yukari Hayashi; Masato Ohashi; Sensuke Ogoshi

To be cited as: Chem. Asian J. 10.1002/asia.201601313

Link to VoR: http://dx.doi.org/10.1002/asia.201601313

A Journal of

ACES Asian Chemical Editorial Society

A sister journal of Angewandte Chemie and Chemistry – A European Journal

WILEY-VCH

Kinetic and Theoretical Studies on Ni(0)/N-Heterocyclic Carbene-Catalyzed Intramolecular Alkene Hydroacylation

Yoichi Hoshimoto,[a,b] Yukari Hayashi,[a] Masato Ohashi,[a] and Sensuke Ogoshi*[a]

Abstract: A combined kinetic and theoretical study was conducted in order to clarify the details on the reaction mechanism for Ni(0)/I*t*Bu-catalyzed intramolecular alkene hydroacylation. The results confirm the hypothesis that this intramolecular hydroacylation proceeds through an oxanickelacycle key intermediate.

Transition-metal-catalyzed hydroacylation is accepted as a promising synthetic method to form C–C bonds between an aldehyde and unsaturated compounds, such as alkenes and alkynes.[1,2] The mechanism is believed to proceed through an acyl metal intermediate generated by oxidative addition of the aldehyde to the metal center. The acyl metal complex is also proposed as a key intermediate in the transition-metal-catalyzed decarbonylation reactions of aldehydes.[3] Thus, decarbonylation causes a decrement in the yield of the target product in hydroacylation reactions. In order to enhance the efficiency of the hydroacylation process, many strategies have been developed to suppress decarbonylation from the acyl metal intermediate.[4,5] In particular, chelation-assisted systems have significantly progressed, and these systems have become a major strategy in the design of novel hydroacylation systems.

Recently, we developed the first example of Ni(0)/1,3-di-*tert*-butylimidazol-2-ylidene (I*t*Bu)-catalyzed intramolecular hydroacylation (Scheme 1).[6] A variety of five- and six-membered benzocyclic ketones (**2**) were prepared from 1,5- and 1,6-enals (**1**) in good to excellent yields. Remarkably, no decarbonylation was observed under our catalytic conditions, and thus, this Ni(0)/I*t*Bu-catalyzed hydroacylation represents 100% atom efficiency. A plausible reaction mechanism was proposed as shown in Scheme 1 based on the results of preliminary mechanistic studies using *o*-allylbenzaldehyde (**1a**): (i) **C1a** and **(C2a)$_2$** were isolated by stoichiometric experiments; and, (ii) transformation of **(C2a)$_2$** into 2-methylindanone (**2a**) was confirmed under both stoichiometric and catalytic conditions. Herein, we report the additional results obtained by kinetic and theoretical studies, and provide the detailed insights on the reaction mechanism.

Kinetic experiments: Reaction of **1a** (0.40 mol m^{-3}) with Ni(cod)$_2$ (2.0×10^{-2} mol m^{-3}) and I*t*Bu (2.0×10^{-2} mol m^{-3}) in mesitylene at 130 °C was monitored by means of GC. The results are shown in Figure 1a. The rate constants of the disappearance of **1a** (k_S) and the production of **2a** (k_P) were

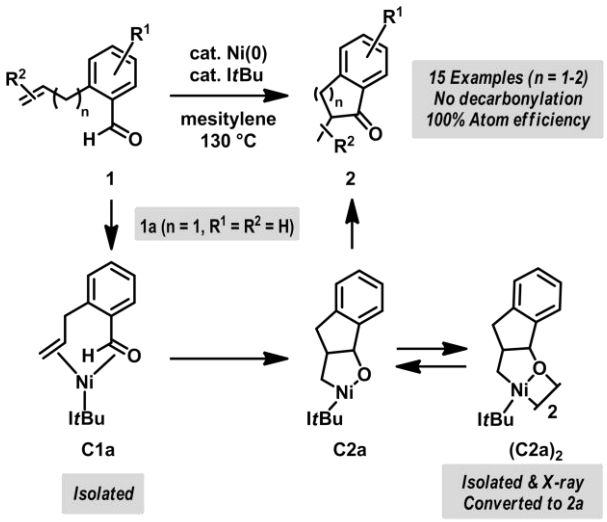

Scheme 1. Ni(0)/I*t*Bu-catalyzed intramolecular alkene hydroacylation. A reaction mechanism previously proposed is shown.

evaluated by the least-squares fitting of the time-concentration profiles to zeroth-order rate equations (Eqs 1 and 2):

$$-d[\mathbf{1a}]/dt = k_S = 3.39(11)\times10^{-5}\ [\text{mol m}^{-3}\ \text{sec}^{-1}] \quad (1)$$

$$d[\mathbf{2a}]/dt = k_P = 2.66(7)\times10^{-5}\ [\text{mol m}^{-3}\ \text{sec}^{-1}] \quad (2)$$

The zeroth-order dependence on [**1a**] indicates that the coordination of **1a** to a Ni(0)/I*t*Bu complex yielding **C1a** is not involved in the rate-determining event. Next, the k_P values were estimated by varying the concentrations of Ni(cod)$_2$ and I*t*Bu from 2.0×10^{-2} to 8.0×10^{-2} mol m^{-3}, giving the profile shown in Figure 1b. Thus, the kinetic order in the Ni/I*t*Bu catalyst is the first order.

Theoretical experiments: Two reaction mechanisms for the hydroacylation of **1a** were evaluated with DFT calculation, which proceeds through (i) oxidative cyclization giving **C2a** (Scheme 2) and (ii) cleavage of the formyl C–H bond giving acyl nickel intermediate **C8a** (Scheme 3). All minima and transition state geometries were optimized with B3PW91 function implemented in Gaussian 09.[7] For calculation of the potential energies, the SDD basis set was used for Ni with an f polarization function, and 6-311+G(d,p) was used for other atoms. The SCRF (mesitylene) with IEF-PCM solvation model was used in all calculations. All relative energies presented herein are Gibbs free energies in kilocalories per mole [kcal mol^{-1}] at 403.15 K with respect to [**Ni(0)/I*t*Bu + 1a**]. Zero-point vibration energies and thermodynamic corrections at 403.15 K were calculated at the same level as the geometry optimization.

[a] Prof. Dr. Y. Hoshimoto, Y. Hayashi, Prof. Dr. M. Ohashi, Prof. Dr. S. Ogoshi
Department of Applied Chemistry, Faculty of Engineering, Osaka University, Suita, Osaka 565-0871, Japan
ogoshi@chem.eng.osaka-u.ac.jp
[b] Prof. Dr. Y. Hoshimoto
Frontier Research Base for Global Young Researchers, Graduate School of Engineering, Osaka University, Suita, Osaka 565-0871, Japan

Supporting information for this article is given via a link at the end of the document.((Please delete this text if not appropriate))

The calculation results on the transformation of **1a** to (η^2-**2a**)Ni(I*t*Bu) (**C6a**) through oxidative cyclization giving oxanickelacycle intermediate **C2a** are shown in Scheme 2. The optimized molecular structures for ***anti*-C1a**, ***trans*-TS1**, ***trans*-C2a**, **TS2**, **C3a**, and **TS4** are also given. Coordination of **1a** to **Ni(0)/I*t*Bu** yields two isomers, ***anti*-C1a** (–29.5 kcal mol^{-1}) and ***syn*-C1a** (–31.5 kcal mol^{-1}), depending on the orientation of the C1–H1 bond with respect to the C5–H5 bond. The molecular

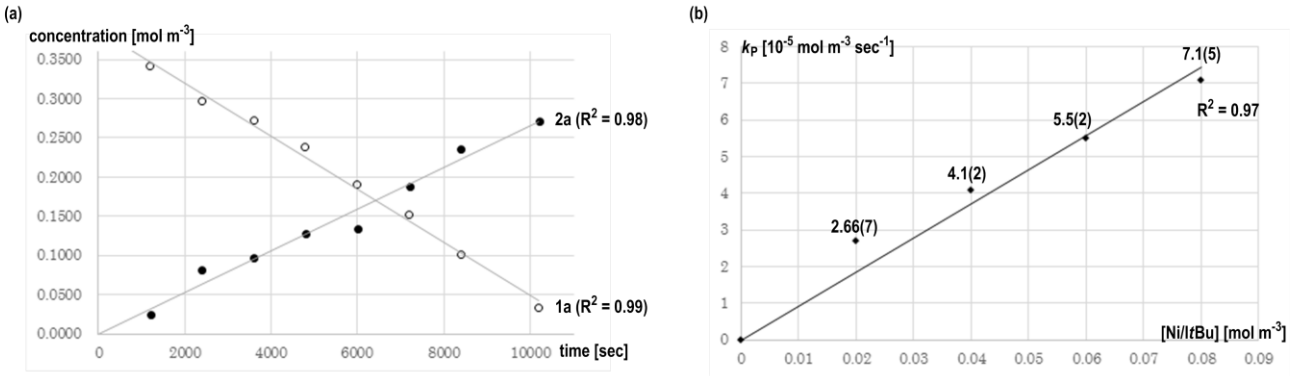

Figure 1. (a) The profile of the concentration of **1a** (○) and **2a** (●) [mol m^{-3}] with respect to reaction time [sec]. Reaction conditions: **1a** (1.59 mmol), Ni(cod)$_2$ (0.080 mmol), and I*t*Bu (0.080 mmol) were reacted in mesitylene (4 mL) at 130 °C. Reaction was monitored by GC using pentadecane as an internal standard. (b) The profile of the concentration of Ni(cod)$_2$/I*t*Bu [mol m^{-3}] with respect to the rate constants of the production of **2a** (k_P) [mol m^{-3} sec^{-1}]. Reaction conditions: (i) [Ni/I*t*Bu] = 0.04 M; **1a** (0.81 mmol), Ni(cod)$_2$ (0.080 mmol), I*t*Bu (0.080 mmol), mesitylene (2 mL) at 130 °C. (ii) [Ni/I*t*Bu] = 0.06 M; **1a** (0.80 mmol), Ni(cod)$_2$ (0.12 mmol), and I*t*Bu (0.12 mmol), mesitylene (2 mL) at 130 °C. (iii) [Ni/I*t*Bu] = 0.08 M; **1a** (1.60 mmol), Ni(cod)$_2$ (0.32 mmol), and I*t*Bu (0.32 mmol), mesitylene (4 mL) at 130 °C. All reactions were monitored by GC using pentadecane as an internal standard.

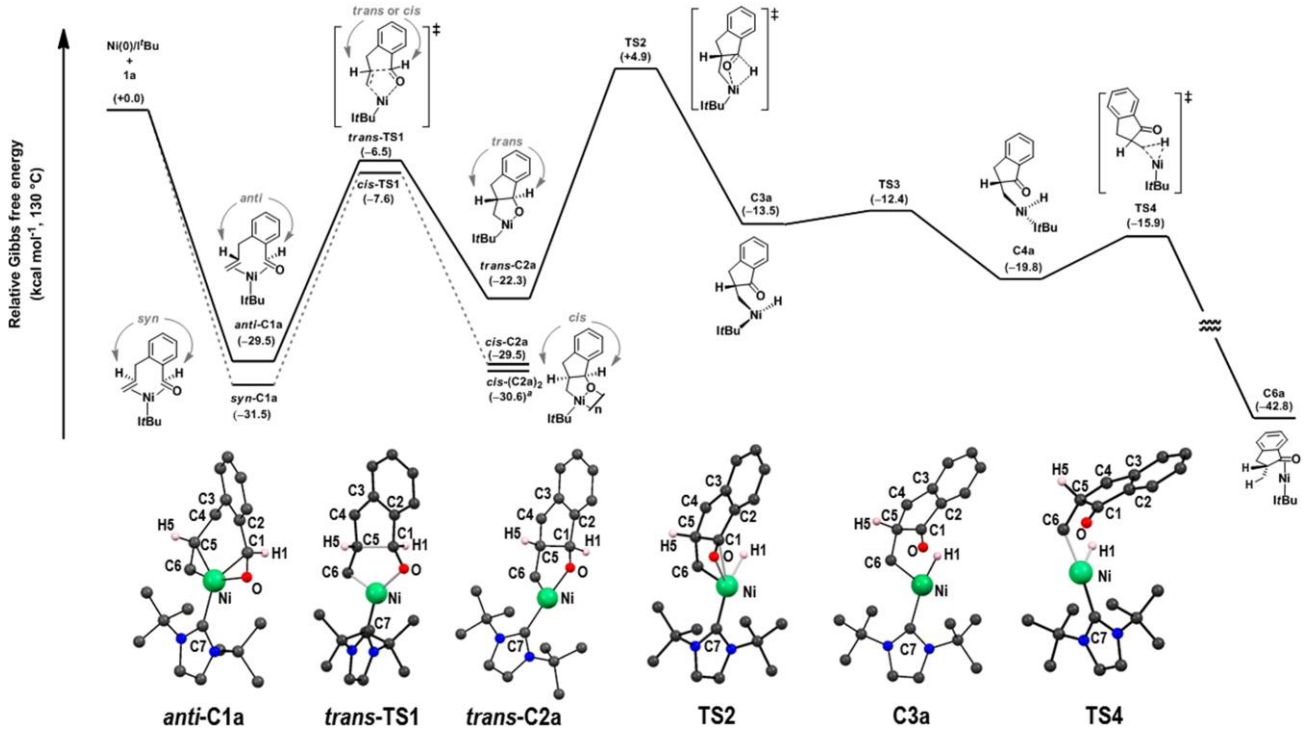

Scheme 2. Gibbs free energy surface of the pathways through oxidative cyclization followed by β-hydride elimination. Relative Gibbs free energies [kcal mol^{-1}] in mesitylene (IEF-PCM solvation model) with respect to [**Ni(0)/I*t*Bu + 1a**] (= +0.0) are shown, calculated by DFT at the B3PW91/SDD(f) for Ni and 6-311+G(d,p) for other atoms (403.15 K). Optimized structures of ***anti*-C1a**, ***trans*-TS1**, ***trans*-C2a**, **TS2**, **C3a** and **TS4** are also given. Hydrogen atoms except H1 and H5 are omitted for clarity. Selected distances [Å] and angles [°]: (***anti*-C1a**) O–Ni 1.96, C1–Ni 1.94, C1•••C5 2.74, C5–Ni 2.03, C6–Ni 2.02, C1–O 1.30, C5–C6 1.40, Ni–C7 1.99; (***trans*-TS1**) O–Ni 1.96, C1•••Ni 2.24, C1•••C5 1.68, C5•••Ni 2.27, C6–Ni 1.88, C1–O 1.37, C5–C6 1.51, Ni–C7 1.85, C6-Ni-O 117.1, C6-Ni-C7 103.3, O-Ni-C7 139.4, O-C1-C5 119.7, C6-C5-C1 114.5; (***trans*-C2a**) O–Ni 1.83, C1•••Ni 2.63, C1–C5 1.52, C5•••Ni 2.67, C6–Ni 1.94, C1–O 1.39, C5–C6 1.52, Ni–C7 1.92, C6-Ni-C7 99.3, C7-Ni-O 169.4, O-Ni-C6 91.0; (**TS2**) O•••Ni 2.36, C1•••Ni 2.22, H1•••Ni 1.56, C1•••H1 1.61, C1–O 1.27, C1–C5 1.57, C5–C6 1.52, C6–Ni 1.93, Ni–C7 1.93, C6-Ni-H1 82.6, C6-Ni-C7 103.6, H1-Ni-C7 163.9; (**C3a**) H1–Ni 1.46, H1•••C6 2.23, Ni–C6 1.90, C7–Ni 2.01, C6-Ni-C7 111.0, C7-Ni-H1 166.9, H1-Ni-C6 82.2; (**TS4**) C6•••H1 1.63, H1–Ni 1.43, C6–Ni 1.91, Ni–C7 1.92, C6-Ni-H1 56.2, C6-Ni-C7 175.1, H1-Ni-C7 126.8. [a] Energy value without BSSE correction (–26.3 kcal mol^{-1} with BSSE).

structure of (η^2:η^2-*o*-homoallylbenzaldehyde)Ni(I*t*Bu) was previously confirmed by X-ray analysis, and the corresponding *syn* orientation was determined.[6a] Oxidative cyclization from ***anti*-C1a** produces monomeric oxanickelacycle ***trans*-C2a** (–22.3 kcal mol^{-1}) through ***trans*-TS1** (–6.5 kcal mol^{-1}), and the activation barrier in this step is thus $\Delta G^{\ddagger}$ = 23.0 kcal mol^{-1}. The interatomic distance between C1 and C5 varies from 2.74 Å in ***anti*-C1a** to 1.52 Å in ***trans*-C2a** through ***trans*-TS1** (C1•••C5 1.68 Å), which shows the formation of the C1–C5 bond during this oxidative cyclization process. The monomeric oxanickelacycle complex ***cis*-C2a** (–29.5 kcal mol^{-1}) and dimeric ***cis*-(C2a)$_2$** (–30.6 kcal mol^{-1} without BSSE correction; –26.3 kcal mol^{-1} with BSSE) are also accessible from ***syn*-C1a** through ***cis*-TS1** (–7.6 kcal mol^{-1}). Thus, the oxidative cyclization to form ***cis*-C2a** (and the following dimerization to give ***cis*-(C2a)$_2$**) could occur easily under the catalytic conditions, which is consistent with the experimental result wherein ***cis*-(C2a)$_2$** was isolated in 88% yield as a precipitation from toluene solution of **C1a** after 33 days at room temperature.[6a] A rational structure for **TS2** (+4.9 kcal mol^{-1}) is found in the β-hydride elimination step from ***trans*-C2a** forming nickel hydride intermediate **C3a** (–13.5 kcal mol^{-1}); however, an activation complex in β-hydride elimination from ***cis*-C2a** was not found under the present calculation conditions. Thus, ***trans*-C2a** is key for the production of **2a**. After the formation of **C3a**, isomerization to **C4a** (–19.8 kcal mol^{-1}) followed by reductive elimination through **TS4** (–15.9 kcal mol^{-1}) affords **C6a**. The overall activation barrier for this reaction mechanism is $\Delta G^{\ddagger}$ = 36.4 kcal mol^{-1}, which is calculated using the steps from ***syn*-C1a** to **TS2**.

The reaction pathways through cleavage of the formyl C–H bond were also evaluated under the same calculation conditions. The results and optimized structures of ***anti*-TS5**, ***anti*-C7a**, ***trans*-TS6**, **C8a**, and **TS7** are shown in Scheme 3, wherein the participation of a ligand-to-ligand hydrogen transfer process through ***cis*-** or ***trans*-TS6** is revealed.[8] First, the formation of ***anti*/*syn*-C1a** occurs followed by a change in the coordination mode of the formyl group from η^2-(κ-C,O) to η^2-(κ-C,H) to give ***anti*-C7a** (–19.2 kcal mol^{-1}) and ***syn*-C7a** (–15.9 kcal mol^{-1}). The optimized molecular structures of ***anti*-TS5** and ***anti*-C7a** illustrate this change in coordination mode from ***anti*-C1a** to ***anti*-C7a** through ***anti*-TS5**. The interatomic distances between Ni to H1 and Ni to O vary from 2.45 to 1.62 Å and from 1.96 to 2.76 Å, respectively, through ***anti*-TS5** (Ni•••H1 1.79 Å, Ni•••O 2.59 Å). A rational transition state for the oxidative addition of the formyl C1–H1 bond in ***anti*/*syn*-C7a** to the Ni(0) center affording a nickel hydride intermediate was not found under the present calculation conditions. Alternatively, the pathways were predicted to proceed through the hydrogen transfer from the η^2-

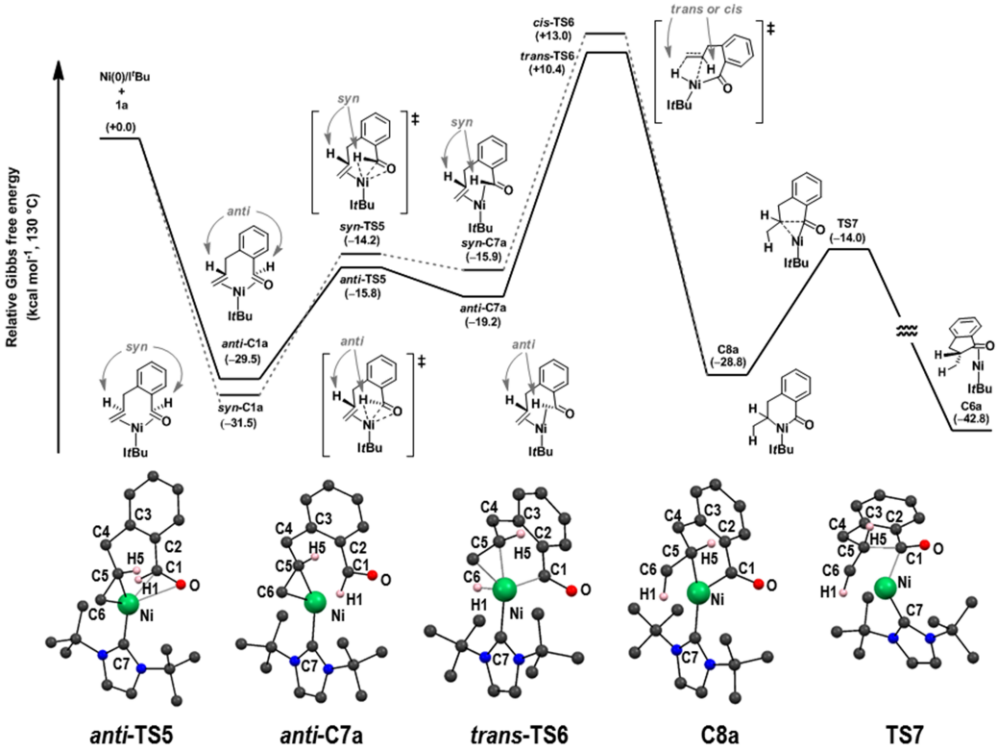

Scheme 3. Gibbs free energy surface of the pathways through cleavage of the formyl C–H bond giving an acyl nickel intermediate. Relative Gibbs free energies [kcal mol^{-1}] in mesitylene (IEF-PCM solvation model) with respect to [**Ni(0)/I*t*Bu + 1a**] (= +0.0) are shown, calculated by DFT at the B3PW91/SDD(f) for Ni and 6-311+G(d,p) for other atoms (403.15 K). Optimized structure of ***anti*-TS5**, ***anti*-C7a**, ***trans*-TS6**, **C8a**, and **TS7** are also given. Hydrogen atoms except H1 and H5 are omitted for clarity. Selected distances [Å] and angles [°]: (***anti*-TS5**) O•••Ni 2.59, C1–Ni 2.08, H1•••Ni 1.79, C1–H1 1.15, C1–O 1.24, C5–Ni 1.99, C6–Ni 1.96, Ni–C7 1.96, Ni-C1-H1 59.2, O-C1-H1 118.2; (***anti*-C7a**) O•••Ni 2.76, C1–Ni 2.01, H1–Ni 1.62, C1–H1 1.22, C1–O 1.24, C5–Ni 1.98, C6–Ni 1.97, Ni–C7 1.96, Ni-C1-H1 53.6, O-C1-H1 115.7; (***trans*-TS6**) O•••Ni 2.87, C1–Ni 2.01, H1–Ni 1.37, C1•••H1 2.73, C6•••H1 2.25, C5–Ni 1.98, C6•••Ni 2.08, Ni–C7 1.94, C1-Ni-H1 106.0, C6-Ni-H1 78.5, C6-Ni-C7 127.7, C7-Ni-C1 104.2, C6-Ni-C1 128.0, C5-Ni-C1 87.1; (**C8a**) C1–Ni 1.84, C5–Ni 1.90, C6•••Ni 2.34, Ni–C7 1.97, C5-Ni-C7 163.9, C7-Ni-C1 109.1, C5-Ni-C1 87.0; (**TS7**) O•••Ni 2.66, C1–Ni 1.88, C1•••C5 1.74, C5•••Ni 2.16, Ni–C7 1.89, C5-Ni-C7 175.2, C7-Ni-C1 127.4, C5-Ni-C1 50.6.

(κ-C,H)-formyl ligand in ***syn-*** or ***anti*-C7a** to the η^2-alkene ligand

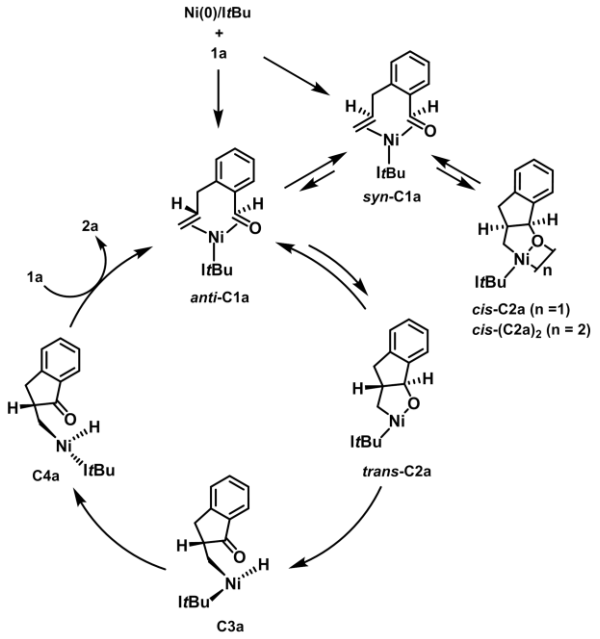

Scheme 4. Detailed catalytic pathways for Ni(0)/I*t*Bu-catalyzed intramolecular hydroacylation of *o*-allylbenzaldehyde **1a**.

through ***cis-*** (+13.0 kcal mol^{-1}) or ***trans*-TS6** (+10.4 kcal mol^{-1}), respectively. As a result, an acyl nickel intermediate **C8a** (–28.8 kcal mol^{-1}) is formed. In the optimized structure of ***trans*-TS6**, the C1–H1 bond is cleaved (C1•••H1 2.73 Å) to form a Ni–H1 bond (Ni–H1 1.37 Å), and then the covalent bonds between C6 and H1, C5 and Ni, and C1 and Ni form simultaneously. From **C8a**, reductive elimination through **TS7** (–14.0 kcal mol^{-1}) furnishes the product **C6a**. Thus, the overall activation barrier is $\Delta G^{\ddagger}$ = 41.9 kcal mol^{-1}, which is given by the steps from ***syn*-C1a** to ***trans*-TS6**.

Given the lower overall activation barrier of 36.4 kcal mol^{-1} for the former vs. 41.9 kcal mol^{-1} for the latter, it is likely that the former pathways proceed through the oxidative cyclization depicted in Scheme 2. Furthermore, this former reaction mechanism is consistent with the following experimental results: (i) the transformation of **1a** to **2a** showed the zeroth- and first-order dependence upon the concentrations of **1a** and Ni/I*t*Bu, respectively; (ii) the isolation of ***cis*-(C2a)$_2$** and its conversion into **C2a** took place under both stoichiometric and catalytic conditions; and, (iii) no decarbonylation was observed under the optimized catalytic conditions.[6a]

Details of the catalytic cycle are summarized in Scheme 4. First, the coordination of **1a** to Ni(0)/I*t*Bu gives ***anti*-C1a** and/or ***syn*-C1a**, in which **1a** coordinates to the Ni(0) center in an η^2-alkene and an η^2-formyl fashion. Under the present calculation conditions, ***syn*-C1a** is predicted to be energetically more stable. The oxanickelacycles ***trans*-C2a** and ***cis*-C2a** are generated from ***anti*-C1a** and ***syn*-C1a**, respectively, through oxidative cyclization processes. The dimeric complex ***cis*-(C2a)$_2$** was previously experimentally isolated;[6a] however, the present calculations show that ***trans*-C2a** is the key intermediate for the production of **2a**. β-Hydride elimination occurs from ***trans*-C2a** to afford nickel hydride intermediate **C3a**. The transition state with the highest relative Gibbs free energy is given in this β-hydride elimination process. Thus, the reaction rate is determined by the pathways from ***syn*-C1a** to **C3a**. Isomerization to **C4a**, reductive elimination, and coordination of **1a** result in a regeneration of ***anti*-C1a** and/or ***syn*-C1a**.

In summary, a combined experimental and theoretical study on the Ni(0)/I*t*Bu-catalyzed intramolecular alkene hydroacylation was performed. Two plausible reaction mechanisms were fully evaluated by DFT calculation. The mechanism proceeding through (i) an oxanickelacycle intermediate given by the oxidative cyclization of η^2-alkene and η^2-formyl ligands on Ni(0) is likely to be compared to the mechanism proceeding through (ii) an acyl nickel intermediate given by a ligand-to-ligand hydrogen transfer from η^2-(κ-C,H)-formyl to η^2-alkene ligands. Kinetic experiments of the reaction showed the zeroth- and first-order dependence on the concentrations of the substrate and the Ni/I*t*Bu catalyst, respectively. All theoretical predictions and experimental results are well consistent with the conclusion that the Ni(0)/I*t*Bu-catalyzed intramolecular hydroacylation of *o*-allylbenzaldehyde proceeds through the oxanickelacycle key intermediate.

Acknowledgements

This work was supported by Grant-in-Aid for Scientific Research (B) (JSPS KAKENHI Grant Number No. 16KT0057), and Scientific Research on Innovative Areas “Stimuli-responsive Chemical Species (No. 2408)” (JSPS KAKENHI Grant Number JP15H00943) and “Precisely Designed Catalysts with Customized Scaffolding (JSPS KAKENHI Grant Number JP15H05803)”. Y.H. acknowledges support from the Frontier Research Base for Global Young Researchers, Osaka University, on the program of MEXT. Y.H. expresses her special thanks for Research Fellowship for Young Scientists from JSPS.

Keywords: hydroacylation, nickel, transition metals, homogeneous catalysis

[1] For selected recent reviews on hydroacylation, see: a) M. C. Willis, *Chem. Rev.* **2010**, *110*, 725–748; b) J. C. Leung, M. J. Krische, *Chem. Sci.* **2012**, *3*, 2202–2209; c) I. D. G. Watson, F. D. Toste, *Chem. Sci.* **2012**, *3*, 2899–2919; d) S. K. Murphy, V. M. Dong, *Chem. Commun.* **2014**, *50*, 13645–13649; e) B. Liu, F. Hu, B.-F. Shi, *ACS Catal.* **2015**, *5*, 1863–1881; for a review on intramolecular variants, see: f) Y. Oonishi, M. Mori, Y. Sato, *J. Synth. Org. Chem., Jpn.* **2007**, *65*, 183–193; for a book, see: g) “Activation of C–H Bonds: Catalytic Reactions”: F. Kakiuchi, S. Murai in *Topics in Organometallic Chemistry. Activation of Unreactive Bonds and Organic Synthesis, Vol.3* (Ed.: S. Murai), Springer, New York, **1999**, chapter 3.

[2] For selected examples of Ni(0)-catalyzed hydroacylation, see: a) T. Tsuda, T. Kiyoi, T. Saegusa, *J. Org. Chem.* **1990**, *55*, 2554–2558; b) H. Taniguchi, T. Ohmura, M. Suginome, *J. Am. Chem. Soc.* **2009**, *131*, 11298–11299; c) F. Yang, T. Jin, Y. Yamamoto, *Tetrahedron* **2012**, *68*, 5223–5228; d) L.-J. Xiao, X.-N. Fu, M.-J. Zhou, J.-H. Xie, L.-X. Wang, X.-F. Xu, Q.-L. Zhou, *J. Am. Chem. Soc.* **2016**, *138*, 2957–2960.

[3] a) J. Tsuji, K. Ohno, *Tetrahedron Lett.* **1965**, *6*, 3969–3971; b) J. Tsuji, K. Ohno, *Synthesis* **1969**, 157–169.

[4] For selected examples of chelation-assisted intramolecular alkene hydroacylations, see: a) H. D. Bendorf, C. M. Colella, E. C. Dixon, M. Marchetti, A. N. Matukonis, J. D. Musselman, T. A. Tiley, *Tetrahedron Lett.* **2002**, *43*, 7031–7034; b) Z. Shen, P. K. Dornan, H. A. Khan, T. K. Woo, V. M. Dong, *J. Am. Chem. Soc.* **2009**, *131*, 1077–1091; c) H. D. Bendorf, K. E. Ruhl, A. J. Shurer, J. B. Shaffer, T. O. Duffin, T. L. LaBarte, M. L. Maddock, O. W. Wheeler, *Tetrahedron Lett.* **2012**, *53*, 1275–1277; for selected examples of chelation-assisted intermolecular alkene hydroacylation, see: d) C. P. Lenges, M. Brookhart, *J. Am. Chem. Soc.* **1997**, *119*, 3165–3166; e) K. Kokubo, K. Matsumasa, M. Miura, M. Nomura, *J. Org. Chem.* **1997**, *62*, 4564–4565; f) M. von Delius, C. M. Le, V. M. Dong, *J. Am. Chem. Soc.* **2012**, *134*, 15022–15032; g) J. F. Hooper, R. D. Young, A. S. Weller, M. C. Willis, *Chem. Eur. J.* **2013**, *19*, 3125–3130; h) T. Zhang, Z. Qi, X. Zhang, L. Wu, X. Li, *Chem. Eur. J.* **2014**, *20*, 3283–3288.

[5] For selected recent reviews on organocatalytic alkene hydroacylation, which afford no decarbonylation products, see: a) D. A. DiRocco, T. Rovis, *Angew. Chem. Int. Ed.* **2011**, *50*, 7982–7983; b) K. Hirano, I. Piel, F. Glorius, *Chem. Lett.* **2011**, *40*, 786–791; c) A. T. Biju, N. Kuhl, F. Glorius, *Acc. Chem. Res.* **2011**, *44*, 1182–1195; for selected examples, see: d) J. He, S. Tang, J. Liu, Y. Su, X. Pan, X. She, *Tetrahedron* **2008**, *64*, 8797–8800; e) M. Schedler, D.-S. Wang, F. Glorius, *Angew. Chem. Int. Ed.* **2013**, *52*, 2585–2589.

[6] a) Y. Hoshimoto, Y. Hayashi, H. Suzuki, M. Ohashi, S. Ogoshi, *Angew. Chem. Int. Ed.* **2012**, *51*, 10812–10815; b) Y. Hoshimoto, M. Ohashi, S. Ogoshi, *Acc. Chem. Res.* **2015**, *48*, 1746–1755; For our related works, see: c) S. Ogoshi, M. Oka, H. Kurosawa, *J. Am. Chem. Soc.* **2004**, *126*, 11802–11803; d) S. Ogoshi, T. Arai, M. Ohashi, H. Kurosawa, *Chem. Commun.* **2008**, 1347–1349; e) Y. Hayashi, Y. Hoshimoto, R. Kumar, M. Ohashi, S. Ogoshi, *Chem. Commun.* **2016**, *52*, 6237–6240. See also the related report; f) A. Ghosh, J. A. Walker, Jr., A. Ellern, L. M. Stanley, *ACS Catal*. **2016**, *6*, 2673–2680.

[7] For details of DFT, see Supporting Information.

[8] J. Guihaumé, S. Halbert, O. Eisenstein, R. N. Perutz, *Organometallics* **2012**, *31*, 1300–1314.

COMMUNICATION

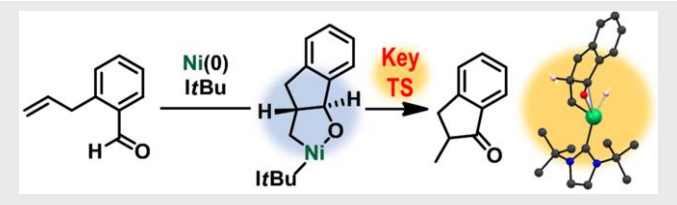

Reaching β-H by twisting: A monomeric and *trans*-nickelacycle intermediate was found to be key for occurrence of the rate-limiting β-H elimination in Ni(0)/I*t*Bu-catalyzed intramolecular alkene hydroacylation, which was revealed by a combined kinetic and theoretical study.

*Yoichi Hoshimoto, Yukari Hayashi, Masato Ohashi, and Sensuke Ogoshi**

Page No. – Page No.

Kinetic and Theoretical Studies on Ni(0)/N-Heterocyclic Carbene-Catalyzed Intramolecular Alkene Hydroacylation